Microfluidic Electrodischarge Devices With Integrated Dispersion Optics for Spectral Analysis of Water Impurities

Long Que, *Member, IEEE*, Chester G. Wilson, *Member, IEEE*, and Yogesh B. Gianchandani, *Senior Member, IEEE*

Abstract—This paper reports a microfluidic device that integrates electrical and optical features required for field-portable water-chemistry testing by discharge spectroscopy. The device utilizes a dc-powered spark between a metal anode and a liquid cathode as the spectral source. Impurities are sputtered from the water sample into the microdischarge and characteristic atomic transitions due to them are detected optically. A blazed grating is used as the dispersion element. The device is fabricated from stacked glass layers, and is assembled and used with a charge-coupled device (CCD) sensing element to distinguish atomic spectra. Two structural variations and optical arrangements are reported. Detection of Cr and other chemicals in water samples has been successfully demonstrated with both devices. The angular resolution in terms of angular change per unit variation in wavelength $(\partial\theta/\partial\lambda)$ is experimentally determined to be approximately 0.10 rad/μm, as opposed to the idealized theoretical estimate of 0.22 rad/μm. This is because the microdischarge is uncollimated and not a point source. However, this is sufficient angular resolution to allow critical spectra of metal impurities to be distinguished. **[1100]**

Index Terms—Chemical sensing, dispersion optics, microdischarge, sample delivery, water chemistry.

I. INTRODUCTION

BIOLOGICAL and chemical threats to our drinking water exist from man-made pollutants and naturally occurring hazards. The evaluation of water quality generally necessitates sampling of the water supply at the site of suspicion, and then transporting the water sample to a laboratory. Inorganic pollutants are typically measured with a plasma spectrometer, which is a relatively large and complex apparatus. Smaller table-top devices, using laser-induced breakdown spectroscopy (LIBS) provide a means for gas, water, and solid chemical detection [1], [2]. These devices rely on a powerful laser to create a plasma that vaporizes the water and its impurities, which are measured spectroscopically. While these devices are smaller than plasma spec-

trometers for water chemistry evaluation, they remain cumbersome for field use. The calibration of these devices also remains a point of some concern, as the measured spectral output provides material specificity, but not concentration for water chemistry applications. A field-portable device would provide a rapid and less expensive means of water testing, and would reduce possible cross contamination of transported samples.

A liquid electrode spectral emission chip (LEd-SpEC) has been reported in the past for detecting inorganic impurities in water [3]. A dc-powered spark between a metal anode and a liquid cathode is used as the spectral source. Impurities are sputtered from the water sample into the microdischarge and characteristic atomic transitions due to them are detected optically. Impurity concentration is found from the ratio of a signature emission strength to that of a reference, such as atmospheric nitrogen, enabling calibration that is not possible with traditional LIBS. However, the original LEd-SpEC chip lacked a proper optical interface. The readout was with an off-chip commercial spectrometer, making it less amenable for simultaneous measurement of multiple samples in a cost-effective manner. In addition, the use of thin-film metal electrodes introduced parasitic resistance that could affect the behavior of microdischarges by suppressing the current peaks, and use of polyimide channels for the liquid sample did not provide a structure that was mechanically as robust and chemically inert as desirable for certain applications. The present effort develops a new device design as well as a new fabrication method with new structural materials and allows a more cost-effective, robust and reliable water chemistry analysis microsystem. The new device also includes on-chip dispersion optics that eliminate the off-chip spectrometer, and permit the chip to be directly read out by a digital camera instead[1]. This is important because it allows the device to be arrayed in parallel for combinatorial analysis. There have been a number of sensor designs (for applications other than water chemistry) that use miniaturized spectrometers for biochemical and infrared sensing [4]–[7]. For all these microspectrometers, a binary grating is utilized as the optical dispersion element, and they all rely on an off-chip, macro-scale optical source. In contrast, the new device utilizes blazed gratings as the dispersion element to maximize the power in the diffraction order of interest. This results in a considerable improvement of the diffraction efficiency of the system, compared to previously reported binary amplitude grating based sensors. Additionally, the on-chip electrodischarge source eliminates the need for an

L. Que was with the Electrical Engineering and Computer Science Department, University of Michigan, Ann Arbor, MI 48109-2122 USA. He is now with Argonne National Laboratory, Center for Nanoscale Materials, Argonne, IL 60439 USA (e-mail: que@anl.gov).
C. G. Wilson was with the Electrical Engineering and Computer Science Department, University of Michigan, Ann Arbor, MI 48109-2122 USA. He is now with Louisiana Tech University, Institute for Micromanufacturing, Ruston, LA 71272 USA (e-mail: chester@latech.edu).
Y. B. Gianchandani is with the Electrical Engineering and Computer Science Department, University of Michigan, Ann Arbor, MI 48109-2122 USA (e-mail: yogesh@eecs.umich.edu).

[1]Portions of these results have been published in conference abstract form in [8].
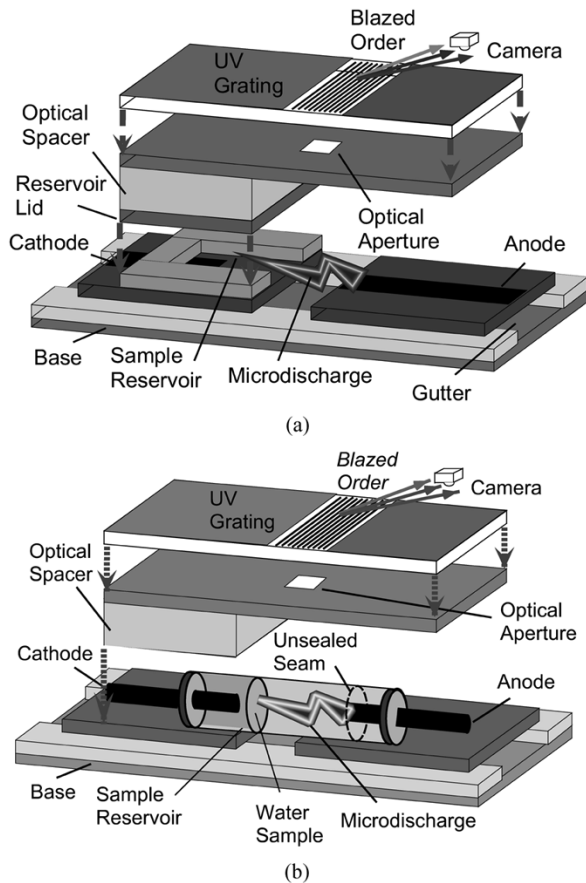
(a)

(b)

Fig. 1. (a) Exploded view of the "*planar*" device. The thick arrows indicate how the system is assembled. (b) Schematic of the "*capillary tube*" device.

Fig. 2. Illustration of a blazed transmission grating.

external laser or plasma. In this effort, we explore the feasibility of using simplified optics, and evaluate the resulting compromises in resolution. The device does not utilize collimation optics, making the implementation compact and portable. The device design is explained in Section II, while the fabrication and experimental results are provided in Sections III and IV, respectively.

II. MICROSYSTEM DESIGN

A. Device Structure

Two versions of the microsystem have been implemented: a "*planar*" and a "*capillary tube*" version. The planar version [see Fig. 1(a)], is multilayer glass device that includes a water sample reservoir, a metal anode, an optical aperture, and a blazed grating. The capillary tube version [see Fig. 1(b)], intended for low-cost, nonlithographic manufacturing, utilizes a glass capillary for the water reservoir and microdischarge. Even though these devices are usually held vertically during operation so that gravity keeps the water sample in place, they can also be held horizontally (as shown) because the high capillary tension secures the water sample. Note that the integrated liquid reservoirs may be a part of a larger microfluidic system with integrated pumps and valves.

An electric discharge is struck between a metal anode and the water sample that is used as the cathode. The water sample
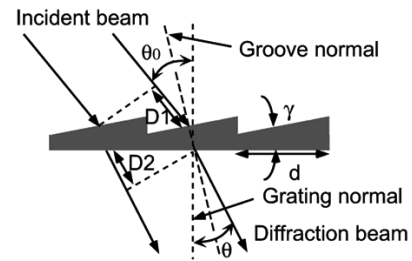
is energized through an immersed metal electrode. Positive ions created in air by the microdischarge bombard the cathodically biased water sample, and sputter the water and metal impurities into the discharge. The metal impurities then emit characteristic spectra, as does the N_2 in the air ambient, which provides a point of comparison for determining the strength of impurity emissions, and hence their concentrations. The tip of the anode is spaced 3 mm from the surface of the energized fluidic electrode. This allows microdischarges to be operated at atmosphere, with a breakdown voltage of 1300 V.

B. Dispersion Optics

The inclusion of dispersion optics within the structure of the device poses a significant challenge. As noted in Section I, previously reported miniaturized spectrometers have been designed for off-chip optical sources, and most of the work has been directed at the long-wavelength end of the spectrum. This particular application calls for a design that is appropriate for on-chip light source that is small but not a point source. Moreover, the spectral content of interest is toward the short wavelength end of the optical spectrum and for some contaminants ranges into the ultra-violet regime. These issues lead to significant challenges in the design of the overall system.

Our initial efforts focused on planar gratings that we fabricated using thin film metal deposited and patterned on a glass substrate. While these were relatively easy to integrate on the system, their performance was inadequate due to various constraints such as material choices for the substrate and the lithographic limitations of available equipment. These gratings were ultimately abandoned in favor of blazed gratings, which offer a more favorable price-to-performance compromise for this microsystem.

Blazed gratings, which are commercially available in sizes adaptable for integration, offer superior diffraction efficiency, which dictates how much of the incident power is converted into useful signal. Maximum (100%) diffraction efficiency occurs when all optical power is delivered to one of the diffraction orders. Blazed gratings are theoretically capable of this, as the geometrical image transmitted through the grooves can be superimposed on a single diffraction order through proper choice of blaze angle [9].

A sketch of a blazed transmission grating is shown in Fig. 2. The direction of diffracted light is governed by the grating equation
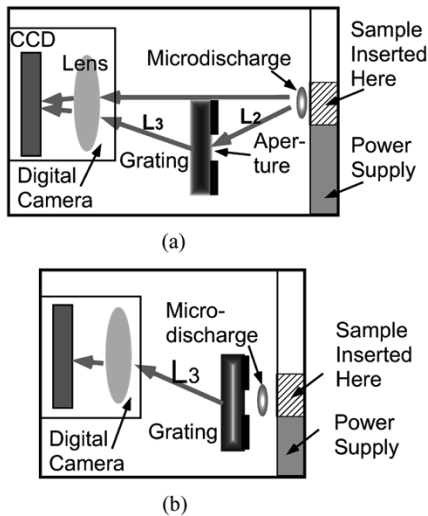
$$m\lambda = d(\sin\theta - \sin\theta_0) \qquad (1)$$

Fig. 3. (a) *Optical configuration I (geometrical version)*, designed to *include* the geometric image of the microdischarge (not to scale). System only requires external camera and power supply for operation. (b) *Optical configuration II (compact version)*, designed to *exclude* the geometric image.
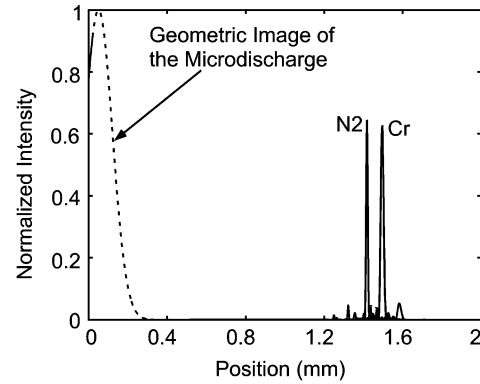

Fig. 4. Calculated spectrum from Cr contaminated water with the geometric image of the microdischarge (dashed line). Configuration in Fig. 3(b) excludes geometrical image.

where θ_0 is the incident angle, θ is the diffraction angle, λ and m are the wavelength and diffraction order and d is the spacing between adjacent grooves on the grating surface (see Fig. 2). If the incident light is *collimated*, each groove of the grating forms an angle γ to the plane of the grating (Fig. 2). For a diffraction grating with N grooves, the diffraction intensity can be described as

$$ I = I_0 \left(\frac{\sin N\phi}{\sin \phi} \right)^2 \left(\frac{\sin \varphi}{\varphi} \right)^2 \qquad (2) $$

where $\phi = (\pi/\lambda)d(\sin\theta - \sin\theta_0)$, $\varphi = (\pi/\lambda)d\cos\gamma \times (\sin(\theta - \gamma) - \sin(\theta_0 - \gamma))$, $2\emptyset$ is the phase difference between the centers of the adjacent grooves (Fig. 2), and φ is the phase difference between the center and edge of a single groove. The second term in (2) is also called the *blaze function* and the relative intensity distribution for a specific incident wavelength can be obtained based on (1)–(2).

An enlarged layout of the optical system, and operational components of the complete system is illustrated in Fig. 3. Two configurations have been evaluated. In configuration I [see Fig. 3(a)], which we have named the *geometrical version*, the microdischarge is separated by a distance L_2 from the aperture using an optical spacer. Under this condition, the external charge-coupled device (CCD) camera can capture the *blazed order* along with the geometric image ("*zeroth*" order) of the microdischarge. The blazed order is formed by constructive interference between a diffraction order and the geometrical image transmitted by the angled grooves. This setup allows the use of the "*zeroth*" and blazed order positions as a reference to calibrate the position of the dispersed wavelengths in the blazed order. However, it needs more space to allow the geometrical image to be captured by CCD camera. Configuration II, which we have named the *compact version*, places the microdischarge in close proximity to the aperture [see Fig. 3(b)], and can utilize a glass spacer as illustrated in Fig. 1. However, with this smaller design, the "*zeroth*" order cannot be captured by the

CCD camera and only the blazed order is captured. In this case, the calibration of the relative positions of different wavelengths has to be performed prior to usage.

There are totally four possible system configurations that result from the two versions of microdischarge source and two optical arrangements: the planar structure with geometrical and compact optical configurations, and the capillary tube version with geometrical and compact optical configurations.

MatLab (MatLab is a trademark of The Math Works, Natick, MA) simulations of both optical systems are shown in Fig. 4. The blazed grating is assumed to have 600 grooves/mm, and a 22° blaze angle. The optical intensity of the microdischarge source is assumed to have a Gaussian profile, with a width of 0.3 mm. In addition, the microdischarge source is assumed to be collimated. The average incident angle θ_0 (Fig. 2) is 5°. The spacing (L_3) between the camera and the grating is 35 cm as used in the experiments. The intensity of the Cr spectra is assumed to be 75% of that of the N_2. The geometrical image size, through lens reduction of the camera, is assumed to be $1/3$ the real size of the microdischarge. The microdischarge is 13 cm (L_2) from the grating for the optical arrangement in Fig. 3(a) and is 2.5 mm for Fig. 3(b). Fig. 4 illustrates that N_2 (with a spectral line at 358 nm) and Cr (425 nm) can be readily distinguished.

Calculations show that the peak positions of the spectra of Cr and N_2 have a 0.15 mm spacing, and the calculated angular resolution $(\partial\theta/\partial\lambda)$ is 0.22 rad/μm for both optical systems. The angular dispersion of the whole system is determined by the grating and the wavelengths of the incident light since the optical arrangements of the CCD camera are fixed. Therefore, the spacing between the spectra of N_2 and Cr on the CCD camera for both optical arrangements shown in Fig. 3 should be the same, and only a function of L_3. As the CCD pixel spacing is 8 μm, an L_3 of only 1.5 cm is required for spectral discrimination. In addition, for the optical system in Fig. 3(a) L_2 can be scaled down from 13 cm to <8 mm, since the only requirement is to ensure the optical path of the microdischarge source is not blocked by the grating, thus can be imaged directly on the CCD sensor. In reality, the microdischarge is un-collimated, so the spectral peaks will be broader, while maintaining the same position.
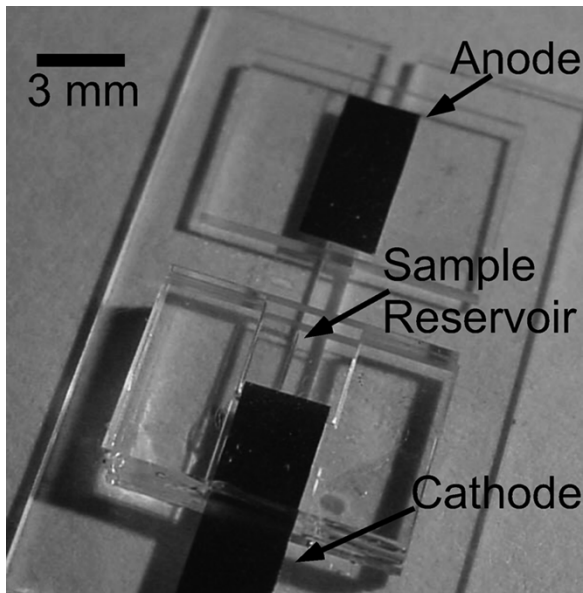
(a)
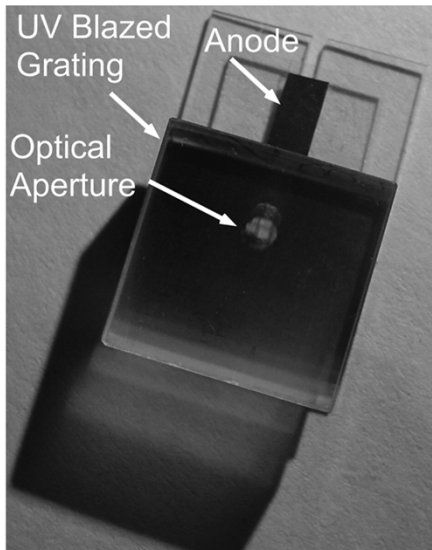
(b)

Fig. 5.   Optical micrographs of a partially assembled (a), and finished planar device (b). Chip area is $\approx 9 \text{ mm} \times 15 \text{ mm}$.

III. FABRICATION

The optical micrographs of a partially complete device with the interior visible and finished planar device are shown in Fig. 5. The fabrication approach selected for this device had to accommodate the goals of mechanical and electrical robustness as well as manufacturability. The device reported in [3] used surface-micromachined polyimide channels and thin-film metal electrodes on a single glass substrate. In contrast, the approach selected for this effort favors a multilayer glass structure with a gutter for improved drainage. The use of polyimide has been completely eliminated. In addition, the metal electrode is now a thick film that is bulk machined from a commercially available planar foil, which is better able to withstand the sputtering of the cathode that can occur if the device is used in an improper
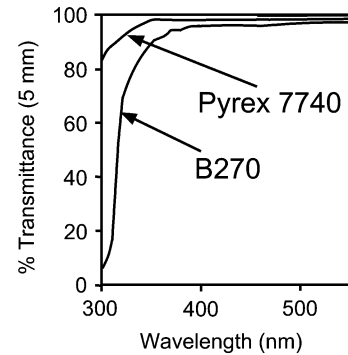

Fig. 6.   Transmission curves for Pyrex #7740 and B270 glass [8].

fashion. A particular consideration in consideration in the fabrication of this device is the method of including the dispersion optics. In the present manifestation of the device, all the structural layers are 506 μm thick, Pyrex #7740 glass except for the top layer, which is a blazed grating with 600 grooves/mm and a 22° blaze angle on 3-mm-thick B270 Schott glass. The #7740 glass substrate is used because of its high transmittance, which is >80% at wavelengths ranging from 300 to 700 nm that are characteristic of metal impurities in water. The transmission curves for both Pyrex #7740 and B270 Schott glass are given in Fig. 6, [10].

For fabricating the water reservoir and discharge source, shown in Fig. 5(a), each layer is processed separately before the stack is bonded together. Ultrasonic machining of thick glass wafers, as reported in the context of wafer-scale packaging [11] provides the necessary throughput and performance for high volume manufacturing of this device. Another option that might be possible for smaller manufacturing volumes is to pick and place rectangular sections of glass into a tiled arrangement in each layer. (This was the approach used for the prototypes.) The fabrication sequence of the microsystem is shown in Fig. 7. This stack consists of seven glass layers. The bottom two layers provide a substrate with a gutter that can drain excess water; the layer above them supports the electrodes, whereas the next two above this form the sidewalls and lid of the sample reservoir. The cathode is the water sample itself, while the anode is constructed from a 30-μm-thick metal film for robustness. The top two layers, which are separated from the rest by a 2.5-mm-thick glass spacer, form the optical dispersion element, including an aperture and diffraction grating [see Fig. 5(b)]. More specifically, the grating is bonded on the lithographically fabricated optical aperture, whereas the optical aperture chip is bonded the water sample chamber through an optical spacer. The detector is a Sony DXC-107 CCD camera. It consists of 768×494 pixels, and each pixel is measured at 8 μm × 9.5 μm.

IV. EXPERIMENTAL RESULTS AND DISCUSSION

Experiments have been performed using both optical systems described in Section II. Fig. 8 shows measured results from the planar structural version of the device [see Fig. 1(a)] using optical configuration I [i.e., the geometrical version, shown in Fig. 3(a)]. The test sample contains Cr contamination. The additional peaks in the region are the result of N_2 spectra. The
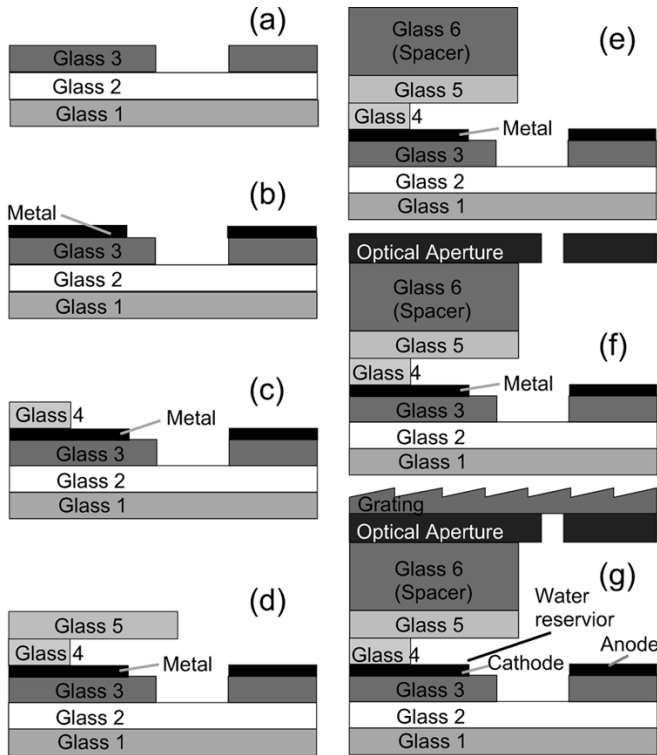
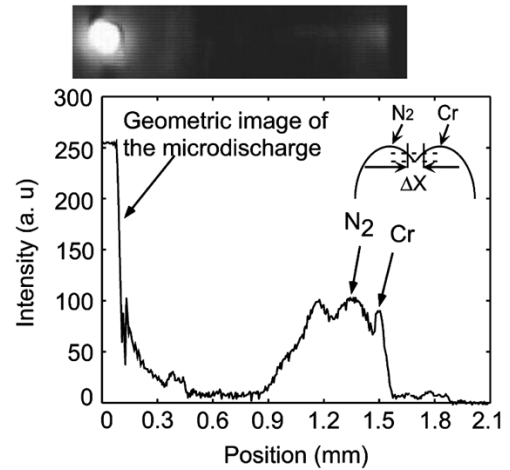Fig. 7. Fabrication sequence of the microsystem.

Fig. 8. Measured diffraction pattern obtained from a Cr contaminated water sample using the planar structure with optical configuration I.
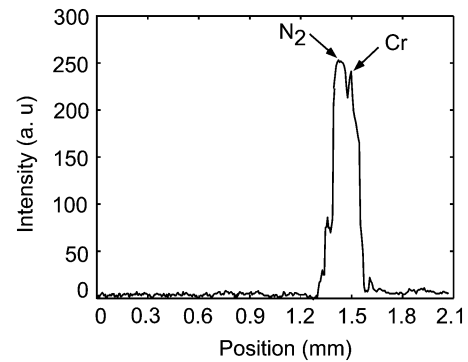

Fig. 9. Measured diffraction pattern from planar structure using Cr contaminated water sample (optical configuration II).
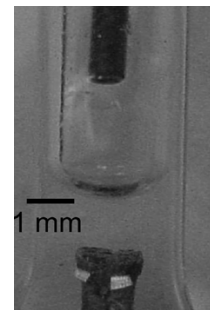

Fig. 10. Close-up of capillary tube with diffraction grating removed, showing microdischarge.

image from the camera is processed using the imaging toolbox in MatLab™ to obtain the relative intensity of the spectra. In contrast to the ideal case, the microdischarge source has nonzero dimensional extent (i.e., it is not a point source), and it is both polychromatic and uncollimated. All of these factors contribute to distortion of the spectral images. The measured angular resolution of the system is reduced to approximately 0.09 rad/μm, which is approximately obtained by

$$\frac{\Delta\theta}{\Delta\lambda} \approx \frac{\Delta X}{F} \times \frac{1}{\Delta\lambda}$$

where $\Delta X = 0.06$ mm is the minimum resolvable spacing between the measured N_2 and Cr spectral peaks. This is defined as the distance formed by the two mid-points in intensity between the respective peaks and their nadir (see insert in Fig. 8). $F = 10$ mm is the effective gap between the CCD array and the focusing lens, and $\Delta\lambda = 67$ nm is the spacing of the characteristic wavelengths for N_2 and Cr. Despite the compromise in performance due to the nonidealities, the diffraction patterns created are clearly distinguishable, which indicates that the angular resolution of the system is more than sufficient to discriminate the spectra of Cr contamination in the water. Fig. 9 shows the spectra generated from the planar structure, with the optical configuration II [of Fig. 3(b)], in which the geometric image is excluded. Again, the N_2 and Cr spectra are clearly separated, illustrating sufficient angular resolution (0.09 rad/μm) of the system. Furthermore, the measured positions and spacing between the spectra of Cr and N_2 [see Figs. 8 and 9] match the simulated predictions.

Fig. 10 shows a close-up view of the microdischarge between the anode and the water sample in the capillary tube version of

the device structure as illustrated in Fig. 1(b). Fig. 11 shows spectra of a Na-contaminated water sample tested in the capillary tube using optical configuration I [i.e., the geometrical version in Fig. 3(a)]. Again, the relevant spectra are distinguishable and the measured angular resolution is approximately 0.11 rad/μm.

For both optical configurations, the spot size of the illumination source is one of the major factors influencing the resolution in the absence of collimating optics. It is found experimentally that the spot size of the microdischarge varies with the spacing between the anode and the cathodically biased water sample, and the shape of the sample reservoir. However, optical
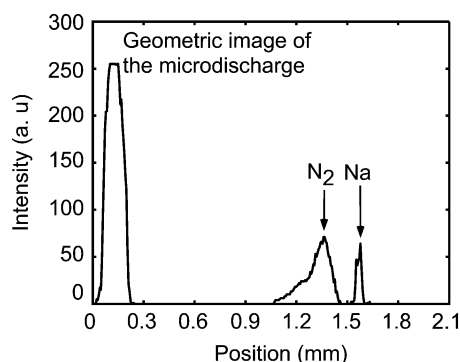
Fig. 11. Measured diffraction pattern obtained with capillary tube plasma using Na contaminated water.

power is sacrificed by reducing the size of the aperture. Since optical power increases the signal-to-noise ratio (SNR), there is a tradeoff between the resolution and optical power.

The integration of collimating optics would improve both the spectral resolution, and would allow lower power operation. The broadening of spectral peaks due to the nonpoint and uncollimated optical source could be mitigated by lenses, which would serve to collect more light, thereby allowing lower power operation of the microdischarge, or a greater signal level. This would come at the expense of a larger and more complex device.

It should be noted that while no attempt was made to evaluate or optimize the sensitivity or specificity of the microsystems, many of the issues discussed above that affect SNR and spectral resolution would relate to these performance parameters. The experiments in this effort were carried out at concentrations in the range of 1–10 part-per-thousand. Prior efforts [3], have shown that concentrations of 1–10 ppm can be detected for various contaminants, although it should be noted that these efforts used a different device structure and larger optics. It is expected that for high sensitivity, this system will be operated with a pre-concentrator as would most other miniaturized chemical sampling systems.

V. CONCLUSION

Two device structures and two optical arrangements of an integrated microsystem for water chemistry analysis have been evaluated in this effort. Attractive features of these systems include an on-chip microdischarge as the optical source and an integrated blazed grating as the dispersion element. The first feature offers the opportunity to make the system more compact and cost effective; the second one improves the diffraction efficiency of the system greatly. In addition, the system can be easily arrayed in parallel for combinatorial analysis. Experiments show that the angular resolution of the whole system is about 0.10 rad/μm compared to the theoretical ideal of 0.22 rad/μm for both planar and capillary version devices because the microdischarge source is uncollimated and is not a point source. However, the Cr and Na contaminants in the water and N_2 spectra from the ambient can be detected readily without

collimation optics, indicating that this angular resolution is sufficient to allow certain spectra to be distinguished.

REFERENCES

[1] J. Kaiser, M. Liska, O. Samek, and P. Knoll, "Characterization of laser-generated micro-plasmas for use in quantitative analysis of liquids," *Proc. SPIE*, vol. 3573, pp. 284–287, 1998.
[2] P. Fichet, A. Toussaint, and J. F. Wagner, "Laser-induced breakdown spectroscopy: A tool for analysis of different types of liquids," *Appl. Phys. A*, vol. A69, pp. 591–592, 1999.
[3] C. G. Wilson and Y. B. Gianchandani, "Spectral detection of metal contaminants in water using an on-chip microglow discharge," *IEEE Trans. Electron Devices*, vol. 49, no. 12, pp. 2317–2322, Dec. 2002.
[4] G. M. Yee, N. Maluf, P. A. Hing, M. Albin, and G. T. A. Kovacs, "Miniature spectrometers for biochemical analysis," *Sens. Actuators A, Phys.*, vol. A 58, pp. 61–66, 1997.
[5] D. Goldman, P. White, and N. Anheier, "Miniaturized spectrometer employing planar waveguides and grating couplers for chemical analysis," *Appl. Optics*, vol. 29, pp. 4583–4589, 1990.
[6] R. Riesenberg, G. Nitzsche, A. Wutting, and B. Harnish, "Micro spectrometer and MEMS for space," in *Proc. 6th ISU Annual International Symposium Small Satellite: Bigger Bussiness?*, Strasbourg, France, May 21–23, 2001.
[7] S. H. Kong, D. L. Wijingaards, and R. F. Wolffenbuttel, "Infrared microspectrometer based on a diffraction grating," *Sens. Actuators A, Phys.*, vol. A 92, pp. 88–95, 2001.
[8] L. Que, C. Wilson, J.-A. E. de La Rode, and Y. B. Gianchandani, "A water spectroscopy microsystem with integrated discharge source, dispersion optics, and sample delivery," in *Technical Digest of 12th Intl. Conf. on Solid-State Sensors, Actuators and Microsystems (Transducers'03)*, 2003, pp. 32–35.
[9] M. Born and E. Wolf, *Principles of Optics*, 7th ed. Cambridge, U.K.: Cambridge University, 1999.
[10] *Product Catalog, Edmund Industrial Optics*, 2001.
[11] B. Ziaie, J. A. von Arx, M. R. Dokmeci, and K. Najafi, "Hermetic glass-silicon micropackage with high-density on-chip feedthroughs for sensors and actuators," *J. Microeletromech. Syst.*, vol. 5, no. 3, pp. 166–179, Sept. 1996.
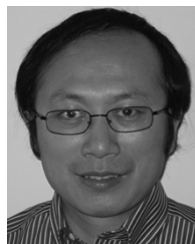
Long Que (M'00) received the undergraduate and graduate education degrees in physics and communication from Peking University, Beijing, China. He received the Ph.D. degree in electrical engineering from the University of Wisconsin-Madison in 2000.

He has held various positions in industry, research institutes, and academia. Currently, he is associated with the Center for Nanoscale Materials at Argonne National Laboratory, Argonne, IL, working on novel integrated nanophotonics for nanoscience, nanotechnology, and biomedical application. Prior to this, he was a Visiting Research Scientist and Research Fellow at the Electrical Engineering and Computer Science (EECS) Department and the Center for Wireless Integrated Microsystems (WIMS) of the University of Michigan, Ann Arbor. His research interests are in bioMEMS/optical/RF/nano MEMS, nanoscience and nanotechnology. He has published more than 20 papers in journals and conferences, has been awarded four U.S. patents, and has several patents pending.

Dr. Que won a National Research Award from the Chinese Academy of Sciences in 1997 and the Vilas Professional Development Fellowship from University of Wisconsin in 2000. He is a Member of SPIE.

Chester G. Wilson (M'03) received the B.S. degree in electrical engineering and the M.S. degree in applied physics from the University of Washington, Seattle, in 1993 and 1996, respectively. In 2002, he received the Ph.D. degree in electrical engineering from the University of Wisconsin, Madison, where he received the Intel Foundation Graduate Fellowship Award.

He was subsequently a Postdoctoral Research Fellow at the NSF Engineering Research Center in Wireless Integrated Microsystems at the University of Michigan, Ann Arbor, and also served as adjunct faculty in the Electrical Engineering and Computer Science (EECS) Department. Since June 2004, he has been an Assistant Professor in the Electrical Engineering Department at the Louisiana Tech. University, Ruston.

Yogesh B. Gianchandani (S'83–M'85–SM'04) received the B.S., M.S., and after some time in industry, the Ph.D. degrees in electrical engineering, with a focus on microelectronics and MEMS.

He is presently an Associate Professor in the Electrical Engineering and Computer Science (EECS) Department at the University of Michigan, Ann Arbor. Prior to this, he was with the Electrical and Computer Engineering (ECE) Department at the University of Wisconsin, Madison. He has also held industry positions with Xerox Corporation, Microchip Technology, and other companies, working in the area of integrated circuit design. His research interests include all aspects of design, fabrication, and packaging of micromachined sensors and actuators and their interface circuits.

Prof. Gianchandani serves on the editorial boards of *Sensors and Actuators, IOP Journal of Micromechanics and Microengineering*, and *Journal of Semiconductor Technology and Science*. He also served on the steering and technical program committees for the IEEE/ASME International Conference on Micro Electro Mechanical Systems (MEMS), and served as a General Co-Chair for this meeting in 2002.